

		Volume 39, December 2013	ISSN 0883-2927
Applied Geochemistry			
JOURNAL OF THE INTERNATIONAL ASSOCIATION OF GEOCHEMISTRY			
Executive Editor Advisory Editor Associate Editors	M. KRSTIC, <i>Malac</i> R. FULF, <i>Aberystwyth</i> L. AGUIRRE, <i>Reims</i> H. ADAMSSON, <i>Reykjavik</i> M. E. AVSTROM, <i>Sweden</i> A. BATH, <i>Loughborough</i> M. BATH, <i>Germany</i> G. BIRN, <i>Germany</i> P. BIRLE, <i>Dhahran</i> S. BOWBELL, <i>Leeds</i> I. CAMPBRIGHT, <i>Clayton</i> A. DAMBERSON, <i>Linköping</i> P. DE CARPIAS, <i>Australia</i> W. M. EDMUNDS, <i>Oxford</i> V. ETTLER, <i>Czech Republic</i> G. FILIPPOLI, <i>Indianapolis</i> D. FORTIN, <i>Ottawa</i>	S. K. FORTNAK, <i>Springfield</i> T. GIMIG, <i>Zurich</i> D. GOSDEN, <i>Wallingford</i> H. M. GUO, <i>China</i> K. HANNA, <i>France</i> J. HOLLOWAY, <i>Lakehead</i> J. ISAK, <i>Sweden</i> A. KOKKER, <i>Reston</i> M. LEVINSOHN, <i>Canada</i> X. D. LI, <i>Kingdon</i> W. B. LYONS, <i>Columbia</i> H. I. MARCINOWSKI, <i>Somerville</i> A. MUKHERJEE, <i>Kharagpur</i> P. NEAUME, <i>France</i> B. NORVINA, <i>Edinburgh</i> D. PARKIN, <i>Canada</i> I. C. PERRY, <i>Gif-Sur-Yvette</i>	E. M. PERCY, <i>USA</i> D. POEYA, <i>Manchester</i> R. M. PEEK, <i>Milano</i> C. REIMANN, <i>Zweilheim</i> J. ROUTH, <i>Linköping</i> E. SACCHI, <i>Italy</i> K. S. SAKAR, <i>Nashville</i> R. R. SHAI, <i>Reston</i> D. B. SMITH, <i>Denver</i> S. STRIEM-GARIVAN, <i>Pittsua</i> A. VENGOSH, <i>Durham</i> P. L. VERPLANCK, <i>Denver</i> B. WANG, <i>Anchorage</i> E. B. WASSY, <i>Denver</i> J. WARRIMAN, <i>Brazil</i>
<p>C. GARING, L. LUQUOT, P.A. PEZARD and P. GOUZE: Geochemical investigations of saltwater intrusion into the coastal carbonate aquifer of Mallorca, Spain 1</p> <p>T. VALENTE, J.A. GRANDE, M.L. DE LA TORRE, M. SANTISTERAN and J.C. CERÓN: Mineralogy and environmental relevance of AMD-precipitates from the Tharsis mines, Iberian Pyrite Belt (SW, Spain) 11</p> <p>E.K. ATIBU, N. DEVARAJAN, F. THEVENON, P.M. MWANAMOKI, J.B. TSHIBANDA, P.T. MPIANA, K. PRABAKAR, J.I. MUREDI, W. WELDI and J. POTE: Concentration of metals in surface water and sediment of Lailu and Musonoie Rivers, Kolwezi-Katanga, Democratic Republic of Congo 26</p> <p>J.M. SORIANO-DISLA, L. JANIK, M.J. McLAUGHLIN, S. FORRESTER, J.K. KIRBY and C. REIMANN, THE EUROGRUSURVEYS GEMAS PROJECT TEAM: Prediction of the concentration of chemical elements extracted by <i>agrus</i> regia in agricultural and grazing European soils using diffuse reflectance mid-infrared spectroscopy 33</p> <p>M. SIGRIST, A. ALBERTENGO, L. BRUNA, H. BELDOMENICO and M. TUDINO: Distribution of inorganic arsenic species in groundwater from Central-West Part of Santa Fe Province, Argentina 43</p> <p>D.B. LOOMER, L. SCOTT, T.A. AL, K. ULRICH MAYER and S. BEA: Diffusion-reaction studies in low permeability shale using X-ray radiography with cesium 49</p> <p>S. BAKEN, C. SJÖSTEDT, J.P. GUSTAFSSON, P. SEUNTIENS, N. DESMET, J. DE SCHUTTER and E. SMOLDERS: Characterisation of hydrous ferric oxides derived from iron-rich groundwaters and their contribution to the suspended sediment of streams 59</p> <p>J. DECLERCQ, O. BOSCH and E.H. OELKERS: Do organic ligands affect forsterite dissolution rates? 69</p> <p>L.E. BERAMENDI-OROSCO, M.L. RODRIGUEZ-ESTRADA, O. MORTON-BERMEA, F.M. ROMERO, G. GONZALEZ-HERNANDEZ and E. HERNANDEZ-ALVAREZ: Correlations between metals in tree-rings of <i>Prosopis juliflora</i> as indicators of sources of heavy metal contamination 78</p> <p>M. DUPUETL, F. VAN HOYE, J. TOUCET and F. GERARD: Citrate adsorption can decrease soluble phosphate concentration in soil: Experimental and modeling evidence 85</p> <p>L. GOURDOL, C. HISSLER, L. HOFFMANN and L. PRIESTER: On the potential for the Partial Triadic Analysis to grasp the spatio-temporal variability of groundwater hydrochemistry 93</p> <p>H. HILLEVANG and P. AAGAARD: Can the long-term potential for carbonatization and safe long-term CO₂ storage in sedimentary formations be predicted? 108</p>			
<i>Continued on outside back cover</i>			

This article appeared in a journal published by Elsevier. The attached copy is furnished to the author for internal non-commercial research and education use, including for instruction at the authors institution and sharing with colleagues.

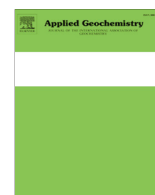
Other uses, including reproduction and distribution, or selling or licensing copies, or posting to personal, institutional or third party websites are prohibited.

In most cases authors are permitted to post their version of the article (e.g. in Word or Tex form) to their personal website or institutional repository. Authors requiring further information regarding Elsevier's archiving and manuscript policies are encouraged to visit:

<http://www.elsevier.com/authorsrights>

Contents lists available at [ScienceDirect](#)

Applied Geochemistry

journal homepage: www.elsevier.com/locate/apgeochem

Arsenic in a fractured slate aquifer system, New England, USA: Influence of bedrock geochemistry, groundwater flow paths, redox and ion exchange



Peter C. Ryan^{a,*}, Jonathan J. Kim^{b,1}, Helen Mango^{c,2}, Keiko Hattori^{d,3}, Ali Thompson^a

^a Geology Department, Middlebury College, Middlebury, VT 05753, USA

^b Vermont Geological Survey, Montpelier, VT 05602-3902, USA

^c Department of Natural Sciences, Castleton State College, Castleton, VT 05735, USA

^d Department of Earth Sciences, University of Ottawa, Ottawa K1N 6N5, Canada

ARTICLE INFO

Article history:

Received 10 April 2013

Accepted 18 September 2013

Available online 4 October 2013

Editorial handling by M. Kersten

ABSTRACT

Elevated As levels have been reported by the Vermont Geological Survey in groundwater from public and domestic bedrock wells in northwestern New England (USA). The study area in southwestern Vermont is underlain by pyrite-rich, organic-rich slates that were thrust over carbonate and clastic sedimentary rocks of the continental shelf during the Ordovician Taconian Orogeny, and the distribution of wells with elevated As shows that they were completed in slates. Hydrochemical and bedrock geochemical analysis indicates that elevated As in the aquifer system is controlled by the following: (1) the presence of black slates that are rich in arsenian pyrite (200–2000 ppm As); (2) release of As via the dissolution of As-rich pyrite; (3) geochemically-reducing and slightly alkaline conditions, where high As values occur at Eh < 200 mV and pH > 7; and (4) physical hydrogeological parameters that foster low Eh and high pH, particularly long groundwater flow paths and low well yields (i.e. high residence time) which provides high rock to water ratios. Where all four factors affect As contents in groundwater, 72% of wells in a zone of distal groundwater flow/low-relief topography exceed 10 µg/L (ppb) and 60% of wells in this zone exceed 25 ppb As. Where flow paths are shorter in slates and groundwater has higher Eh and lower pH (i.e. in regions of higher-relief topography closer to recharge zones), only 3% of wells contain >10 ppb As and none contain >25 ppb.

Overall, 28% (50/176) of low-elevation wells (<245 meters above sea level [masl]) exceed 10 ppb As; only 3% (2/60) of higher-elevation wells (245–600 masl) exceed 10 ppb As. Over the entire aquifer system, 22% of bedrock wells (52/236) exceed 10 ppb and the mean As concentration is 12.4 ppb. Strong positive correlations among Fe, SO₄ and As in groundwater confirm that dissolution of pyrite is the dominant As source. Positive correlations among SO₄, Na and As indicate that, in reducing (Eh < 200 mV) groundwater, Fe(II) is exchanged for Na on mineral surfaces following pyrite dissolution and As remains in solution; conversely, in oxidizing groundwater (recharge zones), Fe(II) is oxidized to Fe(III) and the subsequent formation of ferrihydrite removes As (V) from solution.

© 2013 Elsevier Ltd. All rights reserved.

1. Introduction

Residents of rural regions depend on groundwater for domestic water supply, and in areas with inadequate sand and gravel aquifers, fractured bedrock aquifers are important (Rehbender and Isaakson, 1998; Fernandes and Rudolph, 2001; Ayotte et al.,

2006; Banks et al., 2009; Negrel et al., 2011). One of these regions is the northern Appalachians of New England, where regional surveys indicate that 20–30% of private rural wells may exceed the U.S. Environmental Protection Agency's (USEPA) As maximum contaminant level (MCL) of 10 µg/L (133 nmol/L) (Ayotte et al., 2006). This is a concern because (1) fractured bedrock aquifers are commonly the only reliable source of residential water supply in this region, and (2) consumption of drinking water with elevated As is known to increase risk of bladder cancer, and this may be particularly pertinent in rural New England, where bladder cancer rates exceed rates for the rest of the United States (Brown et al., 1995; Ayotte et al., 2006).

As regional data have emerged in New England (Ayotte et al., 2003, 2006), the need for more-focused, aquifer-specific studies

* Corresponding author. Address: 276 Bicentennial Way, Geology Department, Middlebury College, Middlebury, VT 05753, USA. Tel.: +1 802 443 2557.

E-mail addresses: pryan@middlebury.edu (P.C. Ryan), jon.kim@state.vt.us (J.J. Kim), helen.mango@castleton.edu (H. Mango), khattori@uottawa.ca (K. Hattori), alisonethompson@gmail.com (A. Thompson).

¹ Tel.: +1 802 522 5401.

² Tel.: +1 802 468 1478.

³ Tel.: +1 613 562 5800x6866.

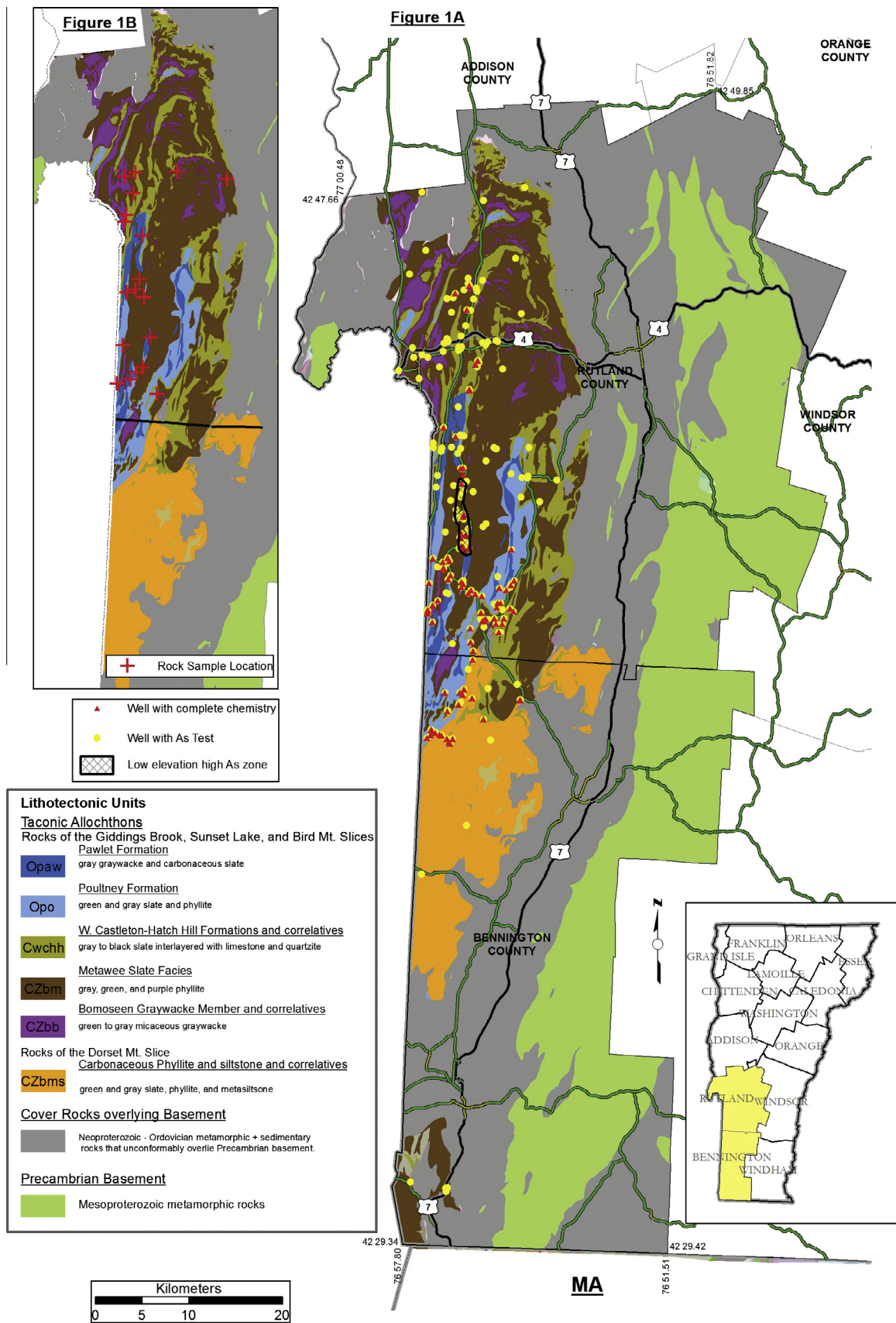


Fig. 1. (A) Location map indicating groundwater sample localities relative to regional bedrock formations, and (B) bedrock sample localities. Geologic map after Ratcliffe et al. (2011).

and predictive models has grown apparent (e.g. Lipfert et al., 2006; Peters and Burkert, 2007; Ryan et al., 2011). The motivation for the current study is as follows: (1) sporadic water testing by residents of the Taconic Mountains region of southwestern Vermont prior to 2010 through the Vermont Department of Health (VDH) revealed that 22 of 55 wells contained greater than 10 µg/L As; (2) in their study of As in groundwater across New England, Ayotte et al. (2006) found that 5 of 6 Taconic region public water supply wells contained As > 10 µg/L; (3) an analysis by the VDH revealed that bladder cancer rates in the Taconic Mountains region, when corrected for smoking, occupation and other factors, are greater than bladder cancer rates for the rest of Vermont (<http://healthvermont.gov/tracking/>); (4) weakly metamorphosed (lower greenschist facies) sedimentary rocks are the most common rock type in fractured bedrock aquifers in New England (Peters, 2008) and are also common globally (e.g. Rehbender and Isaakson, 1998; Fernandes and Rudolph, 2001; Cook, 2003; Banks et al., 2009); and (5) detailed geochemical studies of As and other trace elements in fractured bedrock (or hard-rock) aquifers are sparse, especially when compared to studies of unconsolidated aquifers. These factors indicate that the results of this study have implications for understanding As source and mobility in fractured metasedimentary rock aquifers of New England as well as many other similar aquifers globally.

This paper presents (1) the whole rock geochemistry of the bedrock units of the aquifer system, (2) a detailed hydrochemical survey of wells across the Taconic region of southwestern Vermont, and (3) the relationship between rock geochemistry and groundwater chemistry in order to understand controls on As source and mobility in this system and other aquifers comprised of sedimentary and low grade metasedimentary rocks.

1.1. Geology and hydrogeology of the study area

The bedrock of the Taconic Mountains region of southwestern Vermont (Fig. 1) is dominated by Neoproterozoic to Late Ordovician slates and phyllites with lenses of thinly-bedded carbonate rocks in the lower part of the section (Ratcliffe et al., 2011). These rocks were originally deposited as marine mud on the Laurentian continental slope and rise prior to and during the Taconian Orogeny (Zen, 1972; Landing, 2007; Ratcliffe et al., 2011). Taconic sequence rocks occur discontinuously northward into Quebec and southward into eastern New York State and western Massachusetts and Connecticut. Black and gray slates represent deep marine deposition under dysoxic to anoxic conditions, whereas green and red (or purple) slates were deposited under oxic conditions at relatively shallow depths (Landing, 2007). The middle to late Ordovician Taconian Orogeny (Stanley and Ratcliffe, 1985) created a series of imbricated thrust slices known as the Taconic Allochthon that were emplaced onto Cambrian–Ordovician carbonate and clastic sedimentary rocks of the Laurentian continental shelf; in all, the Taconic allochthon contains seven thrust slices, although only three (the extensive Giddings Brook slice and the neighboring Bird Mountain and Dorset Mountain slices) occur in the field area. The dominant structures (thrusts, folds, fractures, cleavage planes) of the Taconic allochthon are oriented ~north–south, and metamorphic grade slightly increases eastward, from lower chlorite zone in westernmost Vermont (Giddings Brook slice) to upper chlorite zone in the Bird Mountain slice in the easternmost part of the Taconic allochthon in Vermont (for details, see Zen, 1960). Minor modification of Ordovician structures likely occurred during the Devonian Acadian and Permian Alleghenian orogenies (Chan et al., 2000).

The stratigraphy in the Taconic thrust slices is shown in Fig. 1, which is modified from Ratcliffe et al. (2011). Due to the large number of stratigraphic units in the Taconic Allochthon, we consolidated or “lumped” units together based on lithologic similarity,

age, and the associated lithotectonic slice(s). Wherever the stratigraphic unit name in Fig. 1 is modified with “and correlatives”, multiple lithologies were combined for the West Castleton– Hatch Hill Formations, Bomoseen Graywacke Member, and Carbonaceous Phyllite and Siltstone unit.

Groundwater flow in the bedrock aquifer is controlled by the aforementioned N–S structures as well as bedding-parallel fractures and E–W fracture sets (Mango, 2009). Data obtained from the Vermont Online Well Database (http://maps.vermont.gov/imf/jmf.jsp?site=ANR_WSWelldriller) indicates that 93% of the private rural wells in the study area produce from fractured bedrock; the remainder produce from locally thick accumulations of sand and gravel which overlie the bedrock aquifer and vary in appreciably in thickness, grain size and extent. For Taconic region bedrock wells, mean and median static level are 7.4 m and 6.1 m below ground surface, mean (median) well depths are 104 m (96 m), and mean (median) well yield are 38 (19) liters per minute ($L\ m^{-1}$). These wells are unscreened and are open to bedrock over the entire interval other than where steel casing was installed to prevent collapse of unconsolidated overburden at the top of the well. Unconsolidated overburden consists of late Pleistocene sand, gravel and clay, with mean (median) overburden thickness of 15 m (9.6 m); overburden is >30 m thick for 20% of bedrock wells, but in nearly all of these cases it is dominated by silt and clay or compact glacial till.

2. Methods

2.1. Bedrock sampling and analysis

A total of 41 samples of slate bedrock and 10 samples of pyrite-rich slate (>40% pyrite in rock) were collected from the field in 2010 and 2011 for geochemical and petrographic analysis, focusing in particular on areas with clusters of elevated As in bedrock wells (Fig. 1). Given that pyrite predominantly occurs in black, gray and green slates (as compared to quartzites, limestones or purple slates; Landing, 2007), and that preliminary groundwater analyses suggested a positive correlation between As and SO_4 concentrations, pyrite-bearing rock types were targeted for geochemical analysis. Whole-rock compositions were analyzed in two different ways: for samples in the series with prefixes 060210 and 083110, analyses combine inductively coupled plasma-atomic emission spectrometry (ICP-AES) at Middlebury College and ICP-mass spectrometry (ICP-MS) at Acme Analytical Labs (Vancouver, BC, Canada) after fusion with $LiBO_2$ and dissolution in weak HNO_3 . Details of sample preparation and analytical precision are presented in Ryan et al. (2011). Uncertainties determined by replicate analyses and comparison to USGS standard AGV-2 for SiO_2 , Al_2O_3 , Fe_2O_3 and CaO are $\pm 3\%$, whereas for TiO_2 , MnO, MgO, K_2O , Na_2O and P_2O_5 , uncertainties are $\pm 10\%$. Uncertainties for trace elements are $\pm 10\%$ and detection limits are presented in Table S1. The data were normalized to 100% on a post-ignition (i.e. anhydrous, devolatilized) basis, and hence H_2O , CO_2 and S are not included in major element analyses. Samples labeled with a “P” prefix (e.g. P 06-02 B) were analyzed following total digestion by a combination of ICP-MS (after dissolution in HF and HCl) and instrumental neutron activation analysis (INAA) at Actlabs (Toronto, Canada). Seven pyrite-bearing slates were selected for sulfur isotope analysis and were prepared according to methods described in Hattori et al. (2004). Values are presented as ‰ relative to Canyon Diablo Troilite (CDT).

2.2. Groundwater sampling and analysis

Ninety-eight groundwater samples were collected from private rural bedrock wells for this study over a two-year period between

2008 and 2010 (Mango, 2009; Clark et al., 2010). Wells are ~15 cm in diameter and steel-cased through soil and glacial sediments to bedrock; below the bottom of casing, wells are open to the bedrock aquifer. Locations of wells sampled are shown in Fig. 1. Samples were obtained using residential production pumps and if water treatment systems were present, they were bypassed. A calibrated YSI 556 multiprobe was used to measure water temperature, conductivity, pH, oxidation–reduction potential (ORP), and dissolved oxygen (DO) in the field. Samples were collected once all YSI parameters had attained steady values (typically within 5–10 min) and it was apparent that sampled water was being drawn directly from the aquifer. Samples were collected in acid-washed (ultra pure nitric acid), high density polyethylene (HDPE) bottles and stored on ice for delivery to analytical laboratories on the same day, where they were then acidified to a pH < 2 (verified by measuring pH) and filtered with a 0.45 µm filter – this method yields concentrations of total recoverable metals (EPA 3005A) for consumption. Samples were generally clear and lacked visible particulates. ORP measurements were calibrated at 20 °C using ZoBell's solution and then field ORP values were converted to Eh values by adding the difference between the measured ORP of ZoBell's solution and the expected Eh of ZoBell's solution at the temperature of the sample (Nordstrom and Wilde, 2005). Given the temperature range of samples and its effect on ORP–Eh conversion, and stated instrumental precision of ±20 mV (YSI manual), we estimate that precision of reported Eh values is ±30 mV.

Concentrations of metals and anions in groundwater were analyzed in two ways. Samples 121209-1 through 011110-6 (20 samples; Table S2) were analyzed at the Vermont Department of Environmental Conservation Laboratory in Waterbury. Samples for trace metal analysis were acidified with ultra-pure HNO₃ to pH < 2 before analysis, and analytical methods are as follows: ICPMS was used to determine concentrations of metals and metalloids (Al, Sb, As, Ba, Be, Cd, Ca, Cr, Co, Cu, Fe, Pb, Mg, Mn, Mo, Ni, K, Se, Ag, Na, Sr, Tl, U, V, and Zn) according to EPA method 6020; Hg was determined by EPA method 245.1; Cl⁻ was determined by either EPA 300.0 or SM 4500CL-G; SO₄²⁻ and NO₃⁻ were determined by EPA method 300.0; P was determined by SM 4500-PH; SiO₂ by SM 4500 SiO₂-F, and alkalinity by SM 2320B. Detection limits are shown in Table S2. An additional, larger suite of 79 samples (Samples Pwlt DM 1 through Pwlt DM 93 Table S2) were analyzed for a smaller set of analytes by ICP-MS after acidification to pH < 2 (verified by measurement) with concentrated ultra pure nitric acid at Actlabs (Toronto, Canada). Precision and accuracy of analyses were within ±10% (and commonly within 5%) based on replicate analyses and comparison to standards.

Three groundwater samples with elevated As (Table S2) were analyzed for S isotope compositions as follows: groundwater was filtered (0.45 µm) to remove suspended particulates, and the resulting solution was acidified to pH = 1 with 50% HNO₃. Samples were then reacted with BaCl₂ to precipitate BaSO₄ and again acidified to pH = 1 with 50% HNO₃ to dissolve BaCO₃. The samples were then heated to 100 °C for 5 min to dissolve any remaining BaCO₃ and then after cooling BaSO₄ was collected on 0.45 µm filters. SO₂ was released from a mixture of BaSO₄ and V₂O₅ in a Carlo Erba 1110 elemental analyzer at 1700 °C; the SO₂ gas was passed through 7 mL of silica at 1000 °C and Cu at 600 °C and analyzed for δ³⁴S in a Thermo-Finnigan Delta Plus mass spectrometer (University of Ottawa). Values of δ³⁴S (‰) are presented relative to Canyon Diablo Troilite (CDT).

Well depths, static levels, yields, well lithology and overburden characteristics were obtained from a database of well driller reports submitted to the Vermont Department of Environmental Conservation (VDEC). Yields were determined by well driller pump tests that use compressed air from the drill rig as described by the

Massachusetts Department of Environmental Protection (www.mass.gov/dep/water/drinking/wellyld.pdf).

In addition to data reported in Table S2, As concentrations and locations of an additional 138 wells (Fig. 1) were obtained from the Vermont Department of Health, and these data were added to the 98 groundwater samples described above to achieve a larger data set (N = 236) for analysis of the relationship of wellhead elevation and As concentration. Well elevations were determined from GIS contours, and Eh–pH diagrams were made using the “Act2” program and LLNL-Thermo.dat database available in Geochemist's Workbench (Essentials version) (<http://www.gwb.com/>).

3. Results

3.1. Geochemistry and mineralogy of slates in the bedrock aquifer system

Taconic slates are characterized mainly by muscovite, chlorite, quartz and plagioclase with minor pyrite, calcite, dolomite, and in some localities, other low-grade metamorphic minerals such as paragonite, chloritoid, stilpnomelane and zoisite; all samples are within the chlorite zone of the greenschist facies (Zen, 1960) and black slates are rich in organic matter (Landing, 2007), likely bitumen. Major and trace element values (Table S1) are comparable to shale and deep marine clay (Wedepohl, 1978; Rudnick and Gao, 2003). Mean concentration of As in whole-rock for all bedrock samples is 24 mg/kg As, a value that is greater than mean shale or deep marine clay value of 13 mg/kg As (Turekian and Wedepohl, 1961) and the crustal mean of 2 mg/kg (Smedley and Kinniburgh, 2002). In Taconic slates, As contents generally correlate with lithology, and As is particularly enriched in black and gray slates (Fig. 2), where the mean is 95 mg/kg (range = 1.2–971 mg/kg; N = 19). Many of these samples contain visible pyrite (Fig. 3) or weathered relict pyrite with iron hydroxide stain. Green slates, which rarely contain visible pyrite, contain a mean of 6.9 mg/kg As (range = <0.5–24 mg/kg; N = 20) and three purple slates yielded a mean of 3.3 mg/kg As (Table S1). Whereas different types of slate (black-gray vs. green vs. purple) exert a strong control on As concentra-

Period	Formation	Strat. Column	Lithology	As _{WR}	As _{py}
Ordovician	Pawlet Fm		black slate	107 mg/kg	—
	green slate		10 mg/kg	—	
	Mount Merino Fm		purple slate	4.0 mg/kg	—
	Indian River Fm		black slate	196 mg/kg	1100 mg/kg
Cambrian	Poultney Fm		green slate	7.6 mg/kg	—
	West Castleton/ Hatch Hill Fm		black slate	46 mg/kg	379 mg/kg
pC	Bull Fm Mettawee Member		black slate	39 mg/kg	—
			purple slate	3.0 mg/kg	—
			green slate	4.8 mg/kg	—
	Bomoseen & Zion Hill members		purple slate	—	—

Fig. 2. Stratigraphy, lithology, age and average arsenic concentrations in whole rock (As_{WR}) and in pyrites (As_{py}) in Taconic slates (see Tables S2 and 1 for individual analyses). Note high As concentrations in black slates. The Pawlet Fm was locally deposited unconformably on the Poultney, Indian River and Mount Merino formations. The Mount Merino Fm does not occur in the study area and in cases where green and purple slates of the Indian River Formation are thin and discontinuous they have been included in the upper Poultney Formation (Zen, 1964). After Landing (2007) and Ratcliffe et al. (2011).

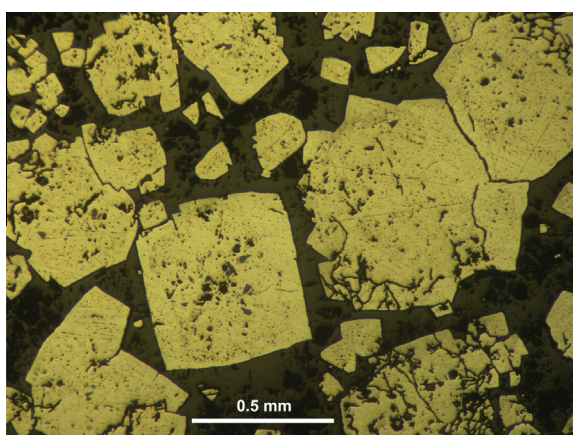


Fig. 3. Thin section photomicrograph of pyrite in a slate cleavage plane (reflected, non-polarized light). Average As concentration in pyrite from this specimen is 728 mg/kg (P 06-10, Table 1).

tion (Fig. 2), there is no appreciable spatial difference in As concentration of slates from north to south in the study area.

3.2. Chemical composition of pyrite

The compositions of ten pyrite-rich slates from the Poultney and West Castleton formations (with >40 wt.% pyrite) are presented in Table 1. We estimated the concentration of As in pyrite from these samples on a post-ignition (devolatilized) basis using % Fe₂O₃(t), total Fe expressed as Fe₂O₃, as a proxy for % pyrite. In this way, As in pyrite (As_{py}) can be estimated as follows (where As_{WR} is As in whole-rock in mg/kg):

$$As_{py} = As_{WR} * 100 / [Fe_2O_3 \text{ wt.\%}]$$

This reveals that the range of As in pyrites sampled from black and gray slates is 236 to 2070 ppm, a range of values similar to those of other early diagenetic and low-grade metamorphic pyrites (Large et al., 2012). One estimation of As in pyrite from a green slate yields low As concentration of 53 ppm.

3.3. Sulfur isotope analysis

Sulfur isotopic compositions of pyrites in black, gray and green slates range from -5.2‰ to +63.0‰ (Tables S1 and 1); average δ³⁴S is +30.1‰ and 11 out of 16 values are greater than +20‰. δ³⁴S values of pyrite are generally proportional to As concentration; for example, pyrite-rich slates with 971 and 993 ppm As had δ³⁴S values of +52.7‰ and +53.5‰ (Table 1), whereas slates with low As (<50 ppm) had δ³⁴S values ≤ +13‰.

Sulfur isotope analysis of SO₄ from three groundwater samples produced values of +26.5‰ (155 ppb As), +18.3‰ (107 ppb As) and +26.2‰ (29.0 ppb As). These values fall within the range of pyrite values (δ³⁴S = +12.9‰ to +52.7‰), consistent with a local pyrite source of dissolved SO₄.

3.4. Arsenic concentration in bedrock wells – geographic and physical factors

Arsenic was detected in all 98 wells (detection limit = 0.03 ppb), and of these, 23.5% (23/98) contain As in concentrations greater than the USEPA MCL of 10 ppb. Mean As concentration in bedrock wells is 12.4 ppb, the range of As in groundwater is 0.03–155 ppb As and the median concentration is 1.4 ppb.

When data are arranged from north to south (Fig. 4A), the northern part of the study area is distinguished by elevated As: 56.8% of

Table 1
Geochemical data of pyrite-rich rock samples (>40% pyrite). All samples contain >20% S and are from the Giddings Brook slice. Major and trace element values are presented on an anhydrous, post-ignition basis.

Sample ID	Fm	Description	SiO ₂ %	TiO ₂ %	Al ₂ O ₃ %	Fe ₂ O ₃ %	MnO %	MgO %	CaO %	Na ₂ O %	K ₂ O %	δ ³⁴ S ‰	As ppm	As _{py} ppm	Cr ppm	Ni ppm	Pb ppm	Th ppm	U ppm	Zn ppm		
P 06-10	Opo	Py cluster in foliation (Fig 3)	0.01	0.01	0.01	0.04	0.01	0.01	0.01	0.01	0.01	39.7	531	728	56	165	374	1.1	0.9	<1		
P 08-06	Opo	Py cubes in black slate	19.3	0.2	2.65	70.9	0.11	0.23	4.11	0.54	0.94	53.5	993	1400	<1	159	235	2.1	<0.5	22		
P 10-10-1A	Opo	Bed-parallel py, black slate	1.6	0.1	1.81	91.8	0.05	0.13	3.44	0.30	0.55	17.3	1020	1111	67	229	226	<0.2	<0.5	9		
P 10-10-1B	Opo	Py crystals in green slate	3.0	0.5	1.70	93.8	0.02	0.12	0.17	0.19	0.48	3.2	49.6	53	244	48	168	104	314	<0.5	25	
P 10-10-1C	Opo	Bed-parallel py, black slate	4.3	0.2	3.25	83.8	0.09	0.17	6.11	0.81	0.92	1050	1253	64	110	29	176	221	<0.2	<0.5	22	
060210-13	Opo	Py cubes, dark gray slate	37.4	0.3	4.76	46.8	0.40	0.52	7.08	1.22	0.94	52.7	971	2074	67	39	93	351	150	NA	46	
P 08-07	Cwchh	Py cubes in black slate	27.9	0.2	6.42	58.0	0.02	0.51	4.18	0.62	2.05	167	288	9	141	32	30	12	2.4	4.4	50	
P 10-10-4B1	Cwchh	Py framboid in black slate	6.5	0.1	1.17	91.5	0.00	0.08	0.07	0.22	0.34	31.4	216	236	6	740	23	15	9	1.3	<0.5	14
P 10-10-4B2	Cwchh	Py cube & fg py, black slate	0.5	0.0	0.68	95.2	0.01	0.10	3.18	0.13	0.17	21.7	303	318	3	275	57	9	<3	<0.2	65	
P 11-10-1	Cwchh	Py cube in gray slate	9.6	0.2	6.61	75.5	0.26	0.53	5.37	0.46	1.45	63.0	509	674	84	46	25	58	302	3.3	<0.5	66

fg = fine-grained; py = pyrite. As_{py} is the calculated concentration of As (ppm or mg/kg) in pyrite based on normalizing Fe₂O₃ to 100%; as such, the pyrite As values likely provide minimum concentrations given that not all Fe in whole-rock occurs in pyrite.

wells (21/37) in the northern Taconics (north of NAD northing 4805000, Fig. 1) contain >10 ppb As, whereas only 3.3% (2/61) in the southern Taconics contain >10 ppb. Mean and median concentrations of As in the northern Taconics are 29.1 ppb and 19.7 ppb, respectively, as compared to only 1.6 ppb and 0.5 ppb in the southern Taconics. Wells with >25 ppb As ($N = 16$, all of which are in the northern Taconics) have mean yield of 34 L min^{-1} , lower than the mean yield for wells with <25 ppb As (44 L min^{-1}). In the northern Taconics, low-yield wells (especially those producing < 50 L min^{-1}) correspond to elevated groundwater As (Fig. 4B). There is no correlation between well depth and groundwater As (Table S2).

It is notable that in a segment between 4805000 and 4815000 (Fig. 1A), 72% of wells (18/25) exceed 10 ppb (Fig. 4A), mean As is 40.1 ppb and the median value is 29.0 ppb. These wells occur in a region of low topography adjacent to groundwater discharge zones, particularly in the lowlands adjacent to large lakes (Lake St. Catherine and Lake Bomoseen).

When groundwater As is plotted as a function of wellhead elevation (this was done for the larger dataset of 236 bedrock wells), high As concentrations occur in the groundwaters at low elevations (Fig. 4C), which are common in the northern Taconics (north of NAD83 northing of 4805000). The high-As wells tend to occur in or near valley bottoms, whereas low-As wells are more commonly situated at higher elevations (Figs. 4C and 5). This likely reflects the residence time of water in aquifer bedrock, where groundwater in low topographic positions has flowed the greatest distance and has had greater time to accumulate As (static levels in wells across the region indicate that flow dominantly follows topography). In many cases, wells with elevated As produce from bedrock units with relatively low whole-rock As content (e.g. Mettawee Member of Bull Formation) that are situated down-gradient of high-As formations (e.g. Pawlet, Poultney and West Castleton) (Fig. 5).

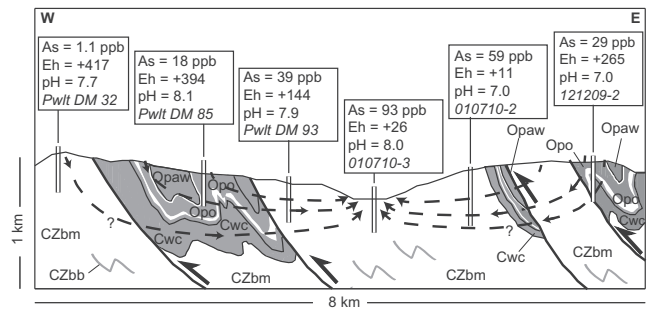


Fig. 5. Schematic cross-section through folded and faulted slates that comprise the Taconic bedrock aquifer system (modified from Ratcliffe et al., 2011). This sketch is intended to emphasize in an idealized way some of the controls on As mobility (wellhead elevation, pH, Eh) as illustrated by six selected wells. Gray units = mainly black and gray slates; white units = mainly green and purple slates. Formation abbreviations correspond to the legend in Fig. 1 (Cwc corresponds to Cwchh on Fig. 1). Dashed arrows indicate general groundwater flow paths but do not indicate details of fracture control, and “?” indicates uncertainty regarding depth of groundwater flow. Units of Eh are mV. Vertical exaggeration = 1.8x.

Northern Taconic groundwaters with >25 ppb As also contain elevated Mn (mean = 109 ppb) relative to southern Taconics groundwaters (mean = 36 ppb Mn; Table S2), a geochemical indicator which is consistent with the presence of lower Eh groundwater in the low-relief northern Taconics (mean Eh = +207 mV) compared to the higher-relief southern Taconics (mean Eh = +405 mV). These relationships likely indicate release of As from Fe and Mn hydroxides under low Eh conditions, but could also be influenced by dissolution of colloidal hydroxides when samples were acidified prior to analysis.

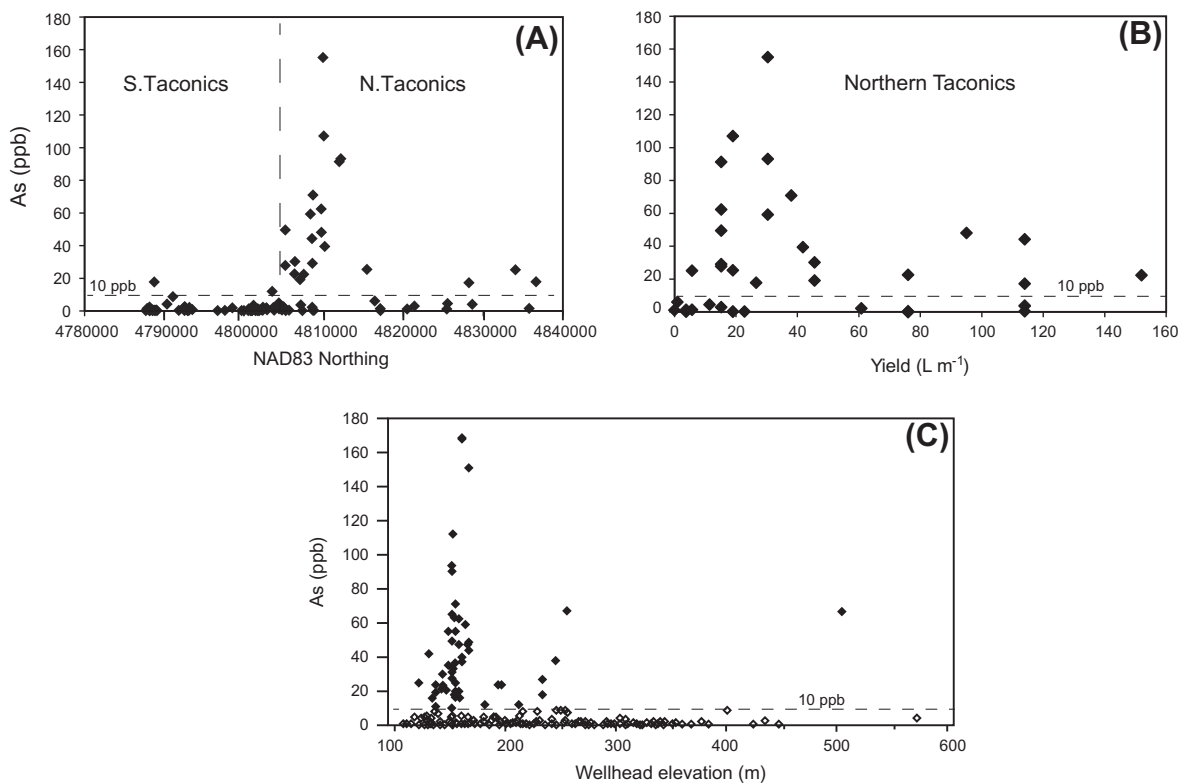


Fig. 4. Relationships between (A) groundwater arsenic concentration along a north–south transect through the study area, (B) well yield (liters per minute) and groundwater arsenic from the northern Taconic region, and (C) elevation of wellheads and As in groundwater from throughout the Taconic region. In general, low yield and low elevation well location result in high As concentrations.

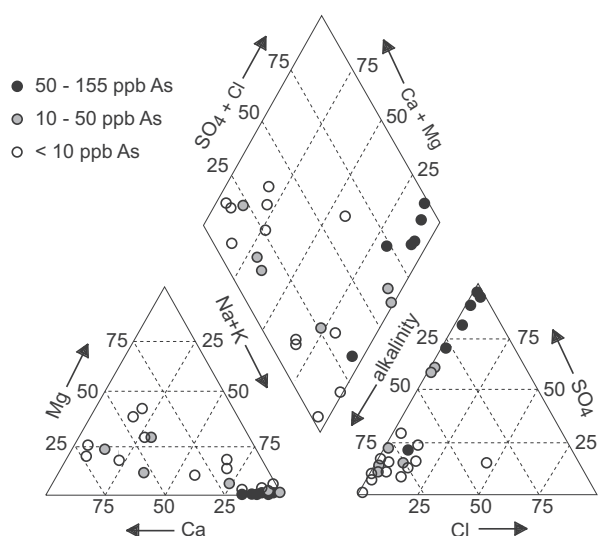


Fig. 6. Hydrochemical facies of groundwater produced from private bedrock wells in the Taconics. Note strong Na-SO₄ signature of high-As wells (>50 ppb) and Ca-HCO₃ signature of low-As wells (<10 ppb).

3.5. Hydrochemical facies

Groundwater samples from the northern Taconics can be divided into two main hydrochemical facies on a Piper plot (Fig. 6): high-As samples with 50–155 ppb As fall predominantly in the Na-SO₄ field, with only one As-rich sample classified as Na-HCO₃; As-poor samples (<10 ppb), on the other hand, are predominantly Ca-HCO₃ or Mg-HCO₃ type. Groundwater samples with intermediate As content (10–50 ppb) generally fall on a mixing line between Na-SO₄ and Ca/Mg-HCO₃. We do not have anion data for the southern Taconics but cation data (Table S2) indicate that these waters tend towards a Ca–Mg signature (rather than Na or K) in nearly all cases, and there is no evidence for a correlation between Na and As in the southern Taconics as there is in the northern Taconics.

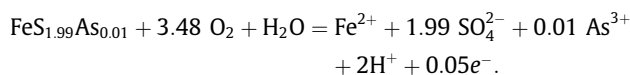
3.6. Arsenic concentration in bedrock wells – hydrochemical controls

Numerous studies indicate that elevated As is common in groundwaters with neutral to basic pH (e.g. Nordstrom, 2002; Peters and Burkert, 2007) and that is generally applicable to the fractured Taconic slate aquifer. Although there is no positive correlation between pH and As, all samples with >10 ppb As occur at a pH ≥ 7.0 and all but one of the high-As samples (>50 ppb) occur at pH > 7.5 (Fig. 7A). This implies that pH = ~7–7.5 is a threshold above which As is desorbed from particulates provided there is an As source, an observation consistent with data from a fractured bedrock aquifer farther to the northeast in New England (Lipfert et al., 2006). The presence of a threshold effect is apparent but less so when analyzing the relationship between Eh and As (Fig. 7B), where low Eh corresponds to elevated As. All As values >25 ppb occur at Eh values ≤ 407 mV and 6 out of 7 As values > 50 ppb occur at Eh ≤ 293 mV. Similar relationships between Eh and As have been noted in aquifers in alluvium (Aziz Hasan et al., 2009) and fractured bedrock (Lipfert et al., 2006; Peters and Burkert, 2007).

The most striking correlations among geochemical parameters are the positive correlations of SO₄–Fe, Fe–As, SO₄–As, SO₄–Na and Na–As (Fig. 7). The following sections (3.6.1 and 3.6.2) examine the roles of reduction–oxidation and ion exchange reactions on the fate and transport of As in this system.

3.6.1. Reduction–oxidation reactions

The linear positive correlation between Fe and SO₄ (Fig. 7C) is strong evidence for oxidation of pyrite in this aquifer system, as described in a pyrite-bearing bedrock aquifer system by Schreiber et al. (2000). Furthermore, the positive correlations of Fe–SO₄, Fe–As and SO₄–As (Fig. 7D and E) indicate that oxidation of arsenian pyrite (via oxidation of S₂²⁻ to 2 S⁶⁺) is the likely source of As, a reaction which can be approximated as:



On a molar basis, the concentration of SO₄ is generally one to two orders of magnitude greater than Fe, indicating either that most Fe is removed from solution following pyrite dissolution, or there is an additional source of SO₄ beyond pyrite; however, given that pyrite is the dominant sulfur-bearing constituent of bedrock in the study area, and that other potential sulfate sources (e.g. gypsum, anhydrite) are unknown in the Taconic sequence (Zen, 1960), the former is far more likely. Iron is most likely reduced in concentration in groundwater by formation of ferrihydrite (or similar poorly crystalline Fe–O–OH phases) and/or exchange of Fe²⁺ or Fe³⁺ for Na⁺ on mineral surfaces (see below).

When the range of compositions of Taconic groundwaters is plotted on an Fe–O–H–S Eh–pH diagram, nearly all samples fall within the fields for Fe²⁺ or Fe(OH)₃ and outside of the stability field for pyrite (Fig. 8); therefore, Eh–pH conditions of the Taconic aquifer system favor oxidation of pyrite. So the likely scenario for release of arsenic entails initial oxidation of arsenian pyrite to Fe²⁺, SO₄²⁻ and As³⁺ (as H₃AsO₃) (Fig. 8) followed by removal of Fe²⁺ from solution by two likely mechanisms: (1) precipitation as ferrihydrite under high pH and Eh conditions (>~0.0 mV); or (2) sorption to mineral surfaces under low Eh conditions (Fig. 9). Consideration of these two processes is covered in Section 3.6.2.

SO₄ generally behaves conservatively in aqueous systems provided it is not reduced to lower oxidation states (e.g. S²⁻), adsorbed onto exchange sites or removed by precipitation into sulfate minerals (Drever, 1997). SO₄ is generally stable at the Eh–pH conditions of the Taconic aquifer system (Eh > –200 mV, pH between 6 and 9) and low Ca and Ba concentrations make sulfate minerals below saturation; also, filtrates from three non-acidified water samples showed no evidence of sulfate minerals by X-ray diffraction analysis, and the only occurrence of sulfates detected was in the form of gypsum along fractures on bedrock exposures where evaporation drives Ca-SO₄ to saturation (Thompson, 2011). Therefore, barring appreciable adsorption to anion exchange sites or microbial conversion to S²⁻, most SO₄ released by pyrite oxidation likely remains in solution and the logarithmic best fit for the SO₄–As correlation (Fig. 7E) indicates that the proportion of As that remains in solution relative to total As released from pyrite decreases with increasing extent of pyrite dissolution. The most likely mechanism of As uptake is sorption onto ferrihydrite or other hydroxides at higher Eh where As occurs as As(V) and higher concentrations of dissolved As will shift the equilibrium toward increased As sorption.

The relative abundances of SO₄ and As released by pyrite oxidation can be estimated given chemical analyses of pyrite-rich rocks (Table 1). For example, pyrite-rich sample 060210-13 contains ~2070 ppm As in pyrite and pyrite contains ~54 wt.% S; therefore, the ratio of S:As in this pyrite (on a mass basis) is 260:1 and SO₄:As is ~780:1, a value which places a lower limit on the SO₄:As ratio given that 060210-13 pyrite is the most As-rich pyrite in this study. Pyrite P 1010-1A contains 1100 ppm As, which would produce a SO₄:As ratio of ~1500, and pyrite in P 10-10-4B(1) contains 236 ppm As, which upon oxidation would yield a SO₄:As ratio of ~2300. In groundwater, the ratio of SO₄:As ranges from 740

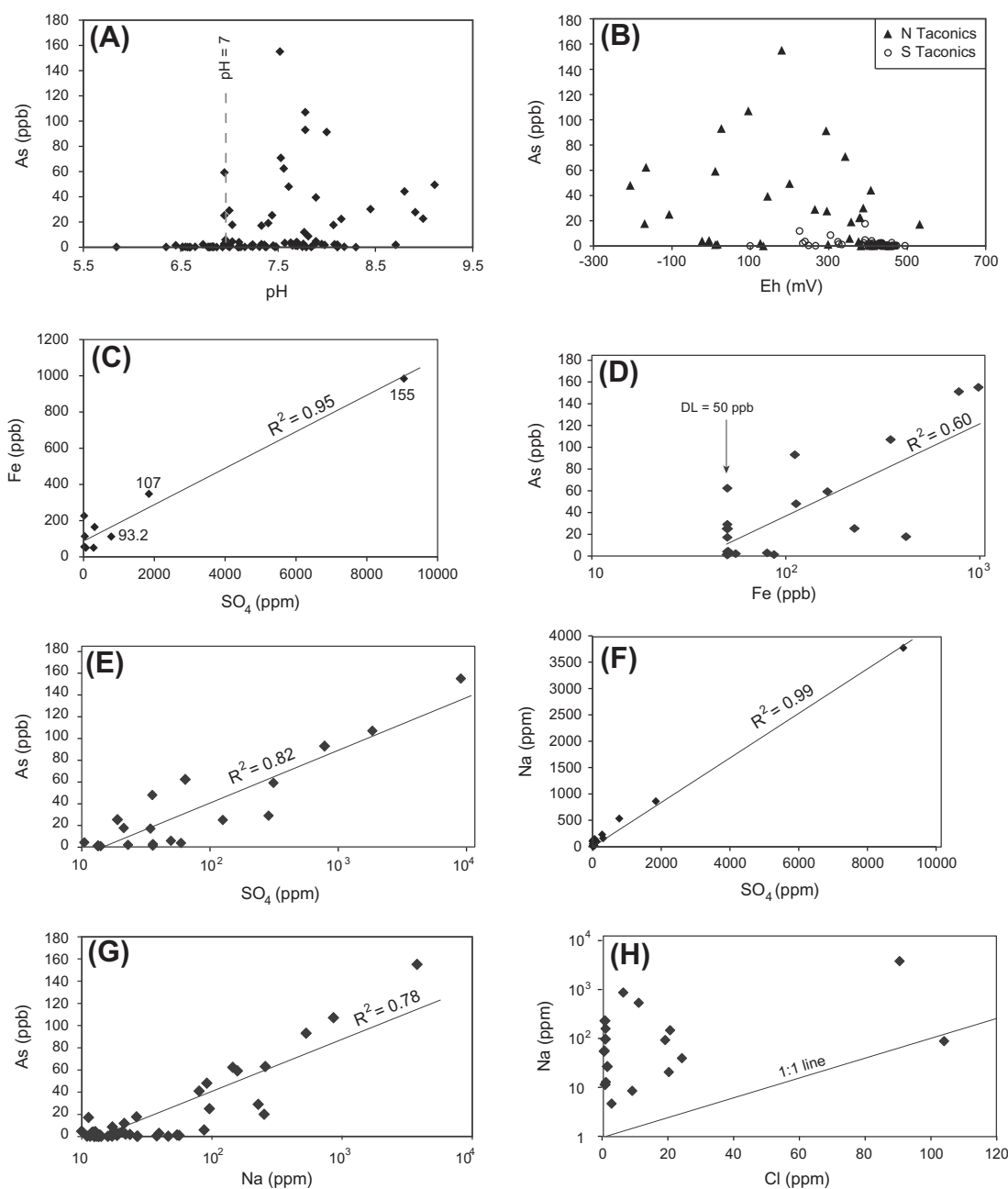
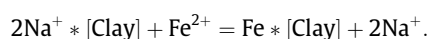


Fig. 7. Bivariate plots of hydrochemical parameters. Values adjacent to points in 7C are arsenic concentrations.

(010810-3) to 58,000 (121209-3), and most values fall between 1000 and 10,000 (based on values in Table S2). Given these values of SO_4 :As in groundwater, and considering that the oxidation of Taconic pyrite would yield SO_4 :As ratios between 780 and 2300 (immediately after dissolution), we can broadly estimate that 25–75% of As released from pyrite is sorbed. The water samples that exhibit the lowest% As sorption, i.e. those with the lowest SO_4 :As ratios (<5500) and highest As content, also have among the lowest Eh values recorded in this study (–206 to +11 mV), indicating that reducing conditions inhibit sorption of As. Low sorption of As in the most-reducing waters is attributed to the instability of Fe-hydroxides and the occurrence of As(III), which is not easily sorbed (Takahashi et al., 2004); conversely, in oxidizing groundwater Fe-hydroxides strongly sorb As as As(V) (Smedley and Kinniburgh, 2002; Dixit and Hering, 2003; Buschmann et al., 2007).

3.6.2. Ion exchange

The positive linear correlation between Na and As ($R^2 = 0.78$; Fig. 7G), and more broadly among Na, As, SO_4 and Fe, suggests that their abundances in solution are linked. The high ratio of Na:Cl in Taconic groundwater (Fig. 7H) rules out road salt or septic effluent as potential Na sources, and the probable source of the elevated Na (as high as 3770 ppm, and with 7 samples >100 ppm) is exchange of Na for divalent cations on surfaces of mica, chlorite or smectite (Fig. 9). Reactions that release Na to solution in exchange for divalent cations, including Fe^{2+} , released by mineral dissolution are known to occur in marine shales and clays (Cerling et al., 1989; Charlet and Tournassat, 2005), and the reaction by which Fe^{2+} replaces Na^+ at an exchange site can be represented as:



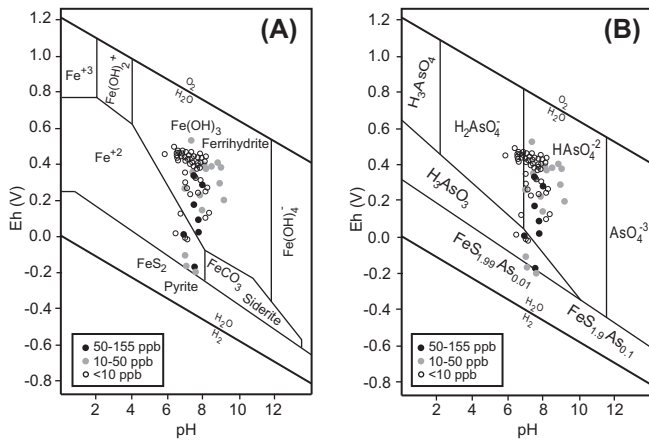


Fig. 8. Eh–pH diagrams at 25 °C and 1 atm. (A) is for Fe–S–O–H–C and (B) is for As–S–O–H–Fe. Circles represent individual groundwater samples. In diagram A, molar concentrations are Fe = 10^{−4} and S species = 10^{−2} and PCO₂ = 10^{−2} atm. Diagram B is based on previous modeling by Saunders et al. (2008), where molar activities of As and S are 10^{−2} and Fe²⁺ is 10^{−8} and there is solid solution between the arsenian pyrite species shown.

In this case, the attraction of divalent Fe²⁺ to negatively-charged surfaces or 2:1 phyllosilicate layers is greater than the attraction of monovalent Na⁺ to these sites, so Fe²⁺ is adsorbed and Na⁺ is released to solution (Fig. 9). The Fe²⁺ is derived from pyrite oxidation, and when Fe²⁺ exchanges for Na⁺, the result is Na⁺ and As in solution, a mechanism which would result in the positive Na–As correlation shown in Fig. 7G.

The persistence of the positive correlation (although not 1:1) of Fe and SO₄ (Fig. 7C) in spite of removal of Fe from solution by ion exchange (or adsorption and precipitation as ferrihydrite or related Fe-hydroxide) may be related to equilibrium exchange reactions (or mineral crystallization) where quantity of Fe²⁺ removed from solution occurs in approximate proportion to its abundance in solution as well as (in the case of ion exchange) competition with other ions (e.g. Ca²⁺) and the composition of ions in exchange sites (e.g. Na⁺). Exchange of Fe²⁺ for Na⁺ can be described by this formulation of the law of mass action:

$$K = a_{\text{Na}^+}^2 * a_{\text{Fe}^{2+}[\text{Clay}]} / a_{\text{Fe}^{2+}} * a_{\text{Na}^+[\text{Clay}]}^2$$

In this scenario, samples with very high initial Fe (e.g. ~500–2500 ppm Fe in conjunction with ~2000–9000 ppm SO₄, assuming congruous pyrite dissolution) will result in large amounts of

exchangeable Na (creating positive correlation of Na–SO₄), while also likely leaving relatively high (e.g. hundreds of ppm) Fe in solution. This type of sample (relatively high Fe, very high SO₄) is one end-member of the Fe–SO₄ correlation, whereas samples with low initial Fe in solution (e.g. ~100 ppm Fe and 400 ppm SO₄), and even lower Fe after exchange or precipitation as hydroxide, will comprise the other end-member of the Fe–SO₄ correlation. In this way, equilibrium exchange can explain the positive (although not 1:1) relationships of Fe and SO₄, and of Na and SO₄. Given that As is released into solution by oxidation of pyrite, it too will maintain a positive correlation with Fe and with SO₄ if its abundance in solution is initially controlled by pyrite dissolution, and then by equilibrium exchange or sorption to Fe-hydroxides proportional to its concentration in solution.

So, to summarize the fates of the products of pyrite dissolution (Fig. 9), SO₄ predominantly remains in solution, while the majority of Fe²⁺ is either exchanged for Na⁺ under reducing, pH-neutral conditions (Eh between −200 and +100 mV and pH ~ 7.5), or is oxidized to Fe³⁺ and precipitated as Fe-hydroxide under more-oxidizing conditions (Eh > +100 mV, pH ~ 7.5). The fate of As liberated by pyrite oxidation appears to be related to: (1) pH, where all As concentrations > 10 ppb occur at pH > 7, and especially at pH > 7.5—this likely relates to desorption of As at slightly alkaline pH (Smedley and Kinniburgh, 2002); and (2) redox conditions and the control exerted by Fe speciation: under the reducing conditions associated with most high-As wells, As is more likely to remain in solution, whereas the oxidizing conditions associated with low-As wells foster sorption of As to ferrihydrite, limiting As mobility. However, of pH and Eh, the former seems to exert a stronger control in this fractured slate aquifer system.

4. Discussion

The general spatial association of As-rich, pyrite-bearing black and gray slates and phyllites with high-As groundwater strongly indicates a bedrock As source. Positive correlations of SO₄–As and Fe–As are consistent with dissolution of As-rich pyrite, and the variability of As concentration in bedrock wells is attributed to proximity to As-rich slate combined with the influence of redox and ion exchange reactions. The potential for an anthropogenic As source is ruled out by a few factors, particularly: (1) the near-absence of NO₃ (≤0.1 ppm in all wells with elevated As), which effectively rules out potential agricultural sources; (2) very low Cl concentrations relative to Na argues against leachfield or road salt sources; and (3) land use history rules out potential contributions from landfill

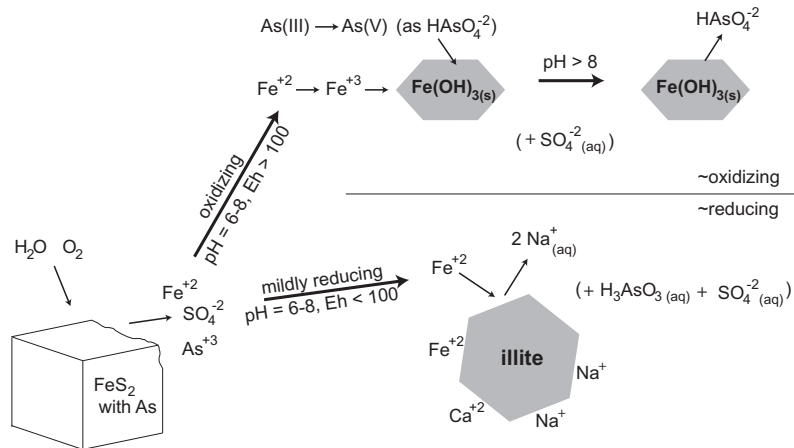


Fig. 9. Schematic diagram illustrating the fates of Fe, As and S upon dissolution of pyrite. Under reducing conditions (like those that dominate northern Taconic groundwater), Fe²⁺ is exchanged for Na⁺ on surfaces of illite or chlorite and As remains in solution. Under oxidizing conditions, Fe²⁺ → Fe³⁺ and formation of Fe-hydroxide sorbs As, limiting As in solution. Units of Eh are mV.

leachate, industrial effluent, lead arsenate insecticide, or other known potential anthropogenic sources.

The elevated As in bedrock of the Taconic aquifer system, particularly in black and gray slates, is attributed to reducing conditions that were periodically present during deposition and early diagenesis of the sediments which are now slates. The Taconic slates originated as marine sediments deposited on the margin of eastern Laurentia (paleo North America) from latest Proterozoic through late Ordovician time (Landing, 2007). Sediments on the continental shelves are known to contain high As (Smedley and Kinniburgh, 2002). In addition, black shales with high contents of organic matter and pyrite typically contain high As (Smedley and Kinniburgh, 2002). The black and gray slates in our samples formed during the periods of anoxia that periodically occurred on the seafloor, especially during late Cambrian through late Ordovician (Landing, 2007), which helps to explain the greater abundance of black-gray slate with elevated As in the late Cambrian to Ordovician West Castleton, Poultney and Pawlet formations (Fig. 2).

Sulfur isotope values of Taconic pyrites, particularly those with $\delta^{34}\text{S} \geq +20\text{‰}$, indicate that pyrite formation occurred with limited supply of open ocean water during periods of anoxia in marine sediments (e.g. Joachimski et al., 2001; Yan et al., 2009); therefore, the anomalously high values of the Taconic pyrites are consistent with extensive reduction of sulfate to sulfide during periods of anoxia or dysoxia in deep marine waters and sediments (Fig. 10). The $\delta^{34}\text{S}$ evidence for extreme anoxia is consistent with stratigraphic and paleontological evidence for dysoxic conditions that accompanied deposition of Taconic black slates during high sea level stands (Landing, 2007), and similarly high $\delta^{34}\text{S}$ values (up to +42‰) occur in pyritized trilobites in anoxic Taconian foreland shales to the west in New York State (Farrell et al., 2009). These strongly reducing conditions resulted in accumulation of organic matter and iron sulfide (e.g. mackinawite, a disordered precursor to pyrite) in black marine muds. Arsenic has an affinity for sulfides and accumulates in early-diagenetic iron sulfide (Large et al., 2012), which resulted in elevated As in the black muds. Subsequent diagenesis and low-grade metamorphism (\leq chlorite grade; Zen, 1960) of Taconic sediment resulted in the arsenian pyrite now present in Taconic black and gray slates (and also to a lesser extent green slates, Tables S1 and 1) and may have further modified $\delta^{34}\text{S}$ values.

Modern-day release of As from pyrite to groundwater is likely initially driven by mildly reducing to oxidizing conditions outside of the stability field of pyrite or arsenian pyrite (Fig. 8); however, while Eh appears to be sufficiently high to oxidize pyrite, it may be too low to foster formation of Fe-hydroxide (Fig. 9), and it is generally in these intermediate conditions where As concentrations are the highest; for example, all high-As samples (>50 ppb) occur in water with Eh < 350 mV (Fig. 8), and low-As (<10 ppb) waters dominate the highest Eh range (~350–500 mV); however, the high Eh range also contains many medium-As (10–50 ppb) samples, emphasizing that Eh is only one of many factors respon-

sible for controlling As mobility and perhaps is less important than pH (Fig. 7A), source rock composition, topographic position and well yield (Fig. 4B and C).

Topographic position (wellhead elevation) and groundwater flow paths influence As content in Taconic groundwater (Figs. 4C and 5). In the low-relief northern part of the study area, wells with elevated As tend to occur in wide valley bottoms and are characterized by relatively low well yields (Fig. 4; Table S2), high Mn and to a lesser extent, low Eh (Fig. 8), parameters which are consistent with slow-moving, chemically-reducing groundwater. These wells are located at the end of groundwater flow paths where weathering of silicates and carbonate has increased pH, pyrite oxidation has consumed O_2 and released As, and increased reaction time contributes to increased As in groundwater—the farther along in the flow path, in general, the higher the pH, the lower the Eh and the higher the As in groundwater (Fig. 5). In contrast, in the southern Taconics, where topography is steeper and wells are closer to recharge areas, groundwater has higher Eh, low As, and lower Fe and Mn. This type of topographic control on As in groundwater has been noted in southeast Asia as well, where Buschmann et al. (2007) found that elevated As in groundwater occurs in areas of low-relief topography where water has low Eh; conversely, areas with higher-relief topography tend to contain high Eh and low As in groundwater.

The results from the Taconic aquifer system may serve as a model for other bedrock aquifers. Metamorphosed sedimentary rocks are the most common rock type in fractured bedrock aquifers in New England (Peters, 2008) and they also comprise bedrock aquifers in many regions globally (e.g. Rehbender and Isaakson, 1998; Fernandes and Rudolph, 2001; Cook, 2003; Banks et al., 2009). Results from the Taconics indicate that lithology, well yield and groundwater age (and hence Eh and pH) strongly influence groundwater As. Black shale and black slate contain pyrite with elevated As and are the main source of As in these rocks; however, young groundwater near recharge zones generally has low As regardless of bedrock As due to low exposure time to rocks, high Eh and ~low pH (i.e. the influence of infiltrated precipitation and soil water is greater). Over time, as groundwater flows down gradient, dissolved oxygen reacts with organic matter, pyrite and other minerals, causing Eh to decrease and pH to increase, and the result is that the highest groundwater As concentrations occur near groundwater discharge zones (wide valley bottoms) due to the confluence of high residence time, low Eh and high pH.

On a societal relevance note, prior to 2009 little was known about the magnitude, extent and origin of As in the Taconic aquifer system – this is when the Vermont Department of Health began to observe repeated high-As results from tests requested by private well owners and, believing that the As source could be geological, requested input from the Vermont Geological Survey. The relative paucity of studies on bedrock aquifers and the results of this study should draw attention to the need for comprehensive testing of

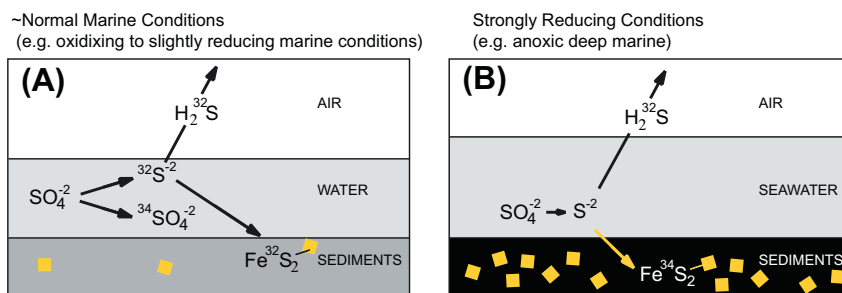


Fig. 10. Fractionation of sulfur isotopes as a function of redox conditions in marine sediments. Loss of ^{32}S in H_2S in strongly reducing conditions results in pyrites with high $\delta^{34}\text{S}$ like those seen in black Taconic slates. Fixation of As into early diagenetic pyrite in highly anoxic sediments resulted in the high As in Taconic slates.

unregulated bedrock wells in bedrock aquifers of all types, particularly those with pyrite-rich black shale or slate.

5. Conclusions

Elevated As in wells of the slate-dominated Taconic bedrock aquifer is influenced by the following features:

- (1) High concentrations of As in pyrites in black and dark gray slates—it is estimated that these pyrites contain 200–2000 mg/kg As.
- (2) Dissolution of As-rich pyrite under oxidizing to mildly reducing conditions in the subsurface.
- (3) pH—elevated As (>10 ppb) only occurs in water with pH > 7.
- (4) To a lesser extent, Eh, which either (a) fosters desorption of As into groundwater in reducing conditions or (b) immobilizes As via sorption to Fe-hydroxides under oxidizing conditions.
- (5) Topography and well yield, where wells in low topographic positions with low yields and pH > 7 correspond to elevated As in groundwater.

Wells with the highest As concentrations, notably those in a low-elevation region where 72% of wells exceed 10 ppb As, occur in areas where all four factors, or a combination of the factors, coincide, i.e. pyrite-rich black slates occurring upgradient of groundwater with low Eh and pH \geq 7 located in low topographic positions. In a region where only one factor occurs (i.e. the southern part of the study area where black slate locally contains elevated As but yields are high, wells are at higher elevations topographically, and groundwater is oxidizing), only 3% of wells exceed 10 ppb As.

Acknowledgements

Gail Center of the Vermont Department of Health observed high-As results in private wells and helped to provide impetus for this study. Arthur Clark and Taylor Smith are thanked for field work, Kate Burchenal and Juliet Ryan-Davis for GIS-based research of the VT well database, and Paul Middlestead for managing the U Ottawa stable isotope lab. Diane Mach also assisted with the project, and we wish to thank all homeowners who allowed us to test their wells. Funding was provided by NSF-EAR-0959306, the Vermont Geological Society, the Middlebury College Undergraduate Research Office, EPSCoR Grant BCD 2004, the Vermont Science Initiative, and Castleton State College.

Appendix A. Supplementary material

Supplementary data associated with this article can be found, in the online version, at <http://dx.doi.org/10.1016/j.apgeochem.2013.09.010>.

References

- Ayotte, J.D., Montgomery, D.L., Flanagan, S.F., Robinson, K.W., 2003. Arsenic in groundwater in eastern New England: occurrence, controls, and human health implications. *Environ. Sci. Technol.* 37, 2075–2083.
- Ayotte, J.D., Bernard, N.T., Nuckols, J.R., Cantor, K.P., Robinson Jr., G.R., Baris, D., Hayes, L., Karagas, M., Bress, W., Silverman, D.T., Lubin, J.H., 2006. Modeling the probability of arsenic in groundwater in New England as a tool for exposure assessment. *Environ. Sci. Technol.* 40, 3578–3585.
- Aziz Hasan, M., Bhattacharya, P., Sracek, O., Ahmed, K.M., von Brömssen, M., Jacks, G., 2009. Geological controls on groundwater chemistry and arsenic mobilization: hydrogeochemical study along an E–W transect in the Meghna basin, Bangladesh. *J. Hydrol.* 378, 105–118.
- Banks, E.W., Simmons, C.T., Love, A.J., Cranswick, R.H., Werner, A.D., Bestland, E.A., Wood, M., Wilson, T., 2009. Fractured bedrock and saprolite hydrogeologic controls on groundwater/surface-water interaction: a conceptual model (Australia). *Hydrogeol. J.* 17, 1969–1989.
- Brown, L.M., Zahm, S.H., Hoover, R.N., Fraumeni, J.F., 1995. High bladder cancer mortality in rural New England (United States): an etiologic study. *Cancer Causes Control* 6, 361–368.
- Buschmann, J., Berg, M., Stengel, C., Sampson, M.L., 2007. Arsenic and manganese contamination of drinking water resources in Cambodia: coincidence of risk areas with low relief topography. *Environ. Sci. Technol.* 41, 2146–2152.
- Cerling, T.E., Pederson, B.L., Damm, K.L.V., 1989. Sodium–calcium ion exchange in the weathering of shales: implications for global weathering budgets. *Geology* 17, 552–554.
- Chan, Y.-C., Crespi, J.M., Hodges, K.V., 2000. Dating cleavage formation in slates and phyllites with the $^{40}\text{Ar}/^{39}\text{Ar}$ laser microprobe: an example from the western New England Appalachians, USA. *Terra Nova* 12, 264–271.
- Charlet, L., Tourmassat, C., 2005. Fe(II)–Na(I)–Ca(II) cation exchange on montmorillonite in chloride medium: evidence for preferential clay adsorption of chloride–metal ion pairs in seawater. *Aquat. Geochem.* 11, 115–137.
- Clark, A., Smith, T., Kim, J., Ryan, P.C., Mango, H., 2010. Elevated arsenic in domestic wells from the Taconic allochthons in southern Vermont. *Geol. Soc. Am. Abs. Prog.* 42, 185.
- Cook, P.G., 2003. A Guide to Regional Groundwater Flow in Fractured Rock Aquifers. CSIRO Land and Water, Glen Osmond, SA, Australia. ISBN 1-74008-233-8. <<http://npsi.gov.au/files/products/river-landscapes/p020312/p020312.pdf>> (accessed 13.11.12).
- Dixit, S., Hering, J.G., 2003. Comparison of arsenic(V) and arsenic(III) sorption onto iron oxide minerals: implications for arsenic mobility. *Environ. Sci. Technol.* 37, 4182–4189.
- Drever, J.I., 1997. *The Geochemistry of Natural Waters: Surface and Groundwater Environments*, third ed. Simon and Schuster, Upper Saddle River, New Jersey, USA.
- Farrell, Ú.C., Martin, M.J., Hagadorn, J.W., Whiteley, T., Briggs, D.E.G., 2009. Beyond Beecher's Trilobite Bed: widespread pyritization of soft tissues in the Late Ordovician Taconic foreland basin. *Geology* 37, 907–910.
- Fernandes, A.J., Rudolph, D.L., 2001. The influence of Cenozoic tectonics on the groundwater-production capacity of fractured zones: a case study in Sao Paulo, Brazil. *Hydrogeol. J.* 9, 151–167.
- Hattori, K.H., Cabri, L.J., Johanson, B., Zientek, M.L., 2004. Origin of placer laurite from Borneo: Se and As contents, and S isotopic compositions. *Mineral. Mag.* 68, 353–368.
- Joachimski, M.M., Ostertag-Henning, C., Pancost, R.D., Strauss, H., Freeman, K.H., Littke, R., Sinnighe Damsté, J., Racki, G., 2001. Water column anoxia, enhanced productivity and concomitant changes in $\delta^{13}\text{C}$ and $\delta^{34}\text{S}$ across the Frasnian–Famennian boundary (Kowala – Holy Cross Mountains/Poland). *Chem. Geol.* 175, 109–131.
- Landing, E.D., 2007. Ediacaran–Ordovician of East Laurentia – geologic setting and controls on deposition along the New York Promontory region. In: Landing, E.D. (Ed.), *Ediacaran–Ordovician of East Laurentia: S.W. Ford Memorial Volume: New York State Museum Bulletin 510*. The University of the State of New York, Albany, New York, pp. 5–24.
- Large, R., Thomas, H., Craw, D., Henne, A., Henderson, S., 2012. Diagenetic pyrite as a source for metals in orogenic gold deposits, Otago Schist, New Zealand. *New Zealand J. Geol. Geophys.* 55, 137–149.
- Lipfert, G., Reeve, A.C., Sidle, W.C., Marvinney, R., 2006. Geochemical patterns of arsenic-enriched groundwater in fractured, crystalline bedrock, Northport, Maine, USA. *Appl. Geochem.* 21, 528–545.
- Mango, H., 2009. Source of arsenic in drinking water and groundwater flow pathways in southwestern Vermont. *Geol. Soc. Am. Abs. Prog.* 41, 8.
- Negrel, P., Pauwels, H., Dewandel, B., Gandolfi, J.M., Mascré, C., Ahmed, S., 2011. Understanding groundwater systems and their functioning through the study of stable water isotopes in a hard-rock aquifer (Maheshwaram watershed, India). *J. Hydrol.* 397, 55–70.
- Nordstrom, D.K., 2002. Worldwide occurrences of arsenic in groundwater. *Science* 296, 2143–2145.
- Nordstrom, D.K., Wilde, F.D., 2005. Reduction–oxidation potential (electrode method) (Version 1.2). In: *National Field Manual for the Collection of Water-Quality Data*, Book 9. U.S. Geological Survey Techniques of Water-Resources Investigations, pp. 1–22. <http://water.usgs.gov/owq/FieldManual/Chapter6/6.5_v.1.2.pdf> (accessed 24.06.13).
- Peters, S.C., 2008. Arsenic in groundwaters in the Northern Appalachian Mountain belt: a review of patterns and processes. *J. Contam. Hydrol.* 99, 8–21.
- Peters, S.C., Burkert, L., 2007. The occurrence and geochemistry of arsenic in groundwaters of the Newark basin of Pennsylvania. *Appl. Geochem.* 23, 85–98.
- Ratcliffe, N.M., Stanley, R.S., Gale, M.H., Thompson, P.J., Walsh, G.J., 2011. *Bedrock Geologic Map of Vermont: U.S. Geol. Survey Scientific Investigations Map 3184*, 3 Sheets, Scale 1:100,000.
- Rehbender, G., Isaakson, A., 1998. Large-scale flow of groundwater in Swedish bedrock. An analytical calculation. *Adv. Water Res.* 21, 509–522.
- Rudnick, R.L., Gao, S., 2003. The composition of the continental crust. In: Rudnick, R.L. (Ed.), *The Crust*. In: Holland, H.D., Turekian, K.K. (Eds.), *Treatise on Geochemistry*, vol. 3. Elsevier-Perigamon, Oxford, pp. 1–64.
- Ryan, P.C., Kim, J., Wall, A.J., Moen, J.C., Corenthal, L.G., Chow, D.R., Sullivan, C.M., Bright, K.S., 2011. Ultramafic-derived arsenic in a fractured bedrock aquifer. *Appl. Geochem.* 26, 444–457.

- Saunders, J.A., Lee, M.-K., Shamsudduha, M., Dhakal, P., Uddin, A., Chowdury, M.T., Ahmed, K.M., 2008. Geochemistry and mineralogy of arsenic in (natural) anaerobic groundwaters. *Appl. Geochem.* 23, 3205–3214.
- Schreiber, M.E., Simo, J.A., Freiberg, P.G., 2000. Stratigraphic and geochemical controls on naturally occurring arsenic in groundwater, eastern Wisconsin, USA. *Hydrogeol. J.* 8, 161–176.
- Smedley, P.L., Kinniburgh, D.G., 2002. A review of the source, behavior and distribution of As in natural waters. *Appl. Geochem.* 17, 517–568.
- Stanley, R.S., Ratcliffe, N.M., 1985. Tectonic synthesis of the Taconian orogeny in western New England. *Geol. Soc. Am. Bull.* 96, 1227–1250.
- Takahashi, Y., Minamikawa, R., Hattori, K.H., Kurishima, K., Kihou, N., Tuita, K., 2004. Arsenic behaviour in paddy fields during the cycle of flooded and non-flooded period. *Environ. Sci. Technol.* 38, 1038–1044.
- Thompson, A.E., 2011. Geochemical and Sulfur Isotope Analysis of Taconic Slates: Implications for Arsenic Source and Mobility in a Bedrock Aquifer System. Unpublished Bachelors Thesis, Middlebury College, Middlebury, Vermont USA, 70 p.
- Turekian, K.K., Wedepohl, K.H., 1961. Distribution of the elements in some major units of the earth's crust. *Bull. Geol. Soc. Am.* 72, 175–192.
- Wedepohl, K.H., 1978. *Handbook of Geochemistry*. Springer-Verlag, Berlin, New York.
- Yan, D., Chen, D., Wang, Q., Wang, J., Wang, Z., 2009. Carbon and sulfur isotopic anomalies across the Ordovician–Silurian boundary on the Yangtze Platform, South China. *Palaeogeogr. Palaeoclimatol. Palaeoecol.* 274, 32–39.
- Zen, E.-A., 1960. Metamorphism of lower Paleozoic rocks in the vicinity of the Taconic Range in west-central Vermont. *Am. Mineral.* 45, 129–175.
- Zen, E.-A., 1972. Some revisions in the interpretation of the Taconic Allochthon in west-central Vermont. *Geol. Soc. Am. Bull.* 83, 2573–2588.